

Technical note

Title: Hip and lower limbs 3D motion tracking using a double-stage data fusion algorithm for IMU/MARG-based wearables sensors[☆]

José Antonio Barraza Madrigal^{a,*}, Lauro Armando Contreras Rodríguez^{b,c,1},
Eladio Cardiel Pérez^{b,2}, Pablo Rogelio Hernández Rodríguez^{b,3}, Humberto Sossa^{d,e,4}

^a Departamento de Formación Básica, Academia de Física, Escuela Superior de Ingeniería Química e Industrias Extractivas ESIQIE-IPN, Instituto Politécnico Nacional, Mexico City, Mexico

^b Center for Research and Advanced Studies of the National Polytechnic Institute, Mexico

^c Facultad de Ciencias Físico-Matemáticas, Universidad Autónoma de Sinaloa, Mexico

^d Instituto Politécnico Nacional, Centro de Investigación en Computación, Laboratorio de Robótica y Mecatrónica, Mexico City, Mexico

^e Tecnológico de Monterrey, Unidad Guadalajara. Zapopan, Jalisco, Mexico



ARTICLE INFO

Keywords:

Hip and lower limbs 3D motion tracking
Orientation of the body segments
Algorithm-based system
MARG sensors
Digital Motion Processor

ABSTRACT

This paper presents an algorithm to estimate the relative orientation of body segments during 3D motion tracking, either as multiple individual body segments or as an articulated body chain. For this purpose, a double-stage data fusion algorithm (algorithm-based system) was implemented for inertial measurement units (IMU)/Magnetic Angular Rate and Gravity (MARG)-based wearable sensors during gait. The methodology considers two stages of complementary filters for the data fusion of the IMU/MARG sensors and a Proportional-Integral controller (PI) to incorporate the processed data. Quaternions were employed for the orientation estimation, a Direction Cosine Matrix quaternion-based (DCM) to estimate the relative orientation between the body mobile coordinate system and the inertial reference coordinate system, and Euler angles for the orientation representation. A customized Ambulatory Sensing Motion System (ASMS), consisting of seven monitoring devices was used for the evaluation. The double-stage algorithm-based system was compared with a digital motion processor (DMP) performance. Experimental results of the double-stage algorithm-based system indicated a 0.7° RMSE (M1) and 1° RMSE (M1-M7) with mean values lower than 1° concerning the DMP outcomes. Based on the Bland-Altman analysis, the level of agreement indicated that the double-stage algorithm-based system is neither underestimated nor overestimated and is suitable for the DMP outcome. No singularity conditions nor significant levels of noise or drift were observed in the conducted experiments. The results demonstrate the feasibility of using the proposed method for 3D human motion tracking of multiple body segments, individually or as an articulated body chain. Besides, it suits different IMU/MARG sensor-based wearable sensors.

[☆] The manuscript has not been published either under consideration for publication elsewhere. All authors substantially contributed to the concept and design of the study, as well as the data acquisition, analysis and interpretation. All authors also drafted and revised the article and approved that the paper was submitted for publication. There are no conflicts of interest to disclose. We hope this revised manuscript is appropriate for publication as a Technical Note in Biomedical Signal Processing and Control Journal.

* Corresponding author at: ESIQIE, Instituto Politécnico Nacional, Edificio 6, Unidad Profesional "Adolfo López Mateos", Col Zacatenco, Delegación, Gustavo A. Madero, Ciudad de México CP. 07738, Mexico

E-mail addresses: jabaraza@ipn.mx (J.A. Barraza Madrigal), armando.contreras@uas.edu.mx (L.A. Contreras Rodríguez), ecardiel@cinvestav.mx (E. Cardiel Pérez), pablo.rogeli@cinvestav.mx (P.R. Hernández Rodríguez), hsossa@cic.ipn.mx (H. Sossa).

¹ Calle Universitarios Ote., Cd. Universitaria, Universitaria, 80010, Culiacán Rosales, Sinaloa, México.

² Electrical Engineering Department/Bioelectronics Section, Av. IPN 2508 Col. San Pedro Zacatenco, Mexico City, Mexico, C.P. 07360.

³ Electrical Engineering Department/Bioelectronics Section, Av. IPN 2508 Col. San Pedro Zacatenco, Mexico City, Mexico, C.P. 07360.

⁴ Av. Juan de Dios Bátiz, Esq. Miguel Othón de Mendizábal, Col. Nueva Industrial Vallejo, Delegación Gustavo A. Madero, Mexico City, Mexico, C.P. 07738.

<https://doi.org/10.1016/j.bspc.2023.104938>

Received 26 October 2022; Received in revised form 18 March 2023; Accepted 5 April 2023

Available online 22 April 2023

1746-8094/© 2023 Elsevier Ltd. All rights reserved.

1. Introduction

3D motion tracking plays an important role in various applications, providing valuable feedback for a better understanding of the human motion condition [1–4]. Many physicians rely on motion tracking devices to assess human motor activity, based on joint kinetics/kinematics and the body segments orientation, to guide diagnosis and improve rehabilitation treatment [5–9]. Due to the extensive range of applications, gait analysis is one of the most evaluated activities, among which stand out health care [10–12], rehabilitation [13], and activities of daily living [14].

Video-based motion analysis systems are widely used for 3D human motion tracking and gait analysis in laboratories and clinical settings [15–17]. However, their use may only sometimes be suitable for motion tracking, especially in assessing the gait motion of daily living activities [18,19]. The main reason is that various factors can affect the images: lighting, foreground focus, and background conditions [19–21]. Furthermore, video-based motion analysis systems require specialized personnel and controlled environments for data capture [22].

The Inertial Measurement Units (IMU)/Magnetic Angular Rate Gravity sensors (MARG) present a feasible solution for tracking human motion in 3D since they allow estimating the kinetics/kinematics and the orientation of a moving object based on physical quantities measurements: angular velocity, gravity vector, and earth's magnetic field [23,24]. Besides, these small and low-cost sensors do not require controlled environments or external references to measure, making them suitable for 3D human motion tracking applications [25,26] and gait analysis [1,27,28].

The use of IMU/MARG sensor for estimating the orientation remains a challenge, mainly due to measurement errors, such as high noise levels and drift, inherent to using these sensors [29]. Integration of gyroscope noise measurements could cause drift in a long-term tracking [9]. Accelerometers are sensitive to body accelerations under dynamic motion conditions. Also magnetometers suffer from variations in the local earth's magnetic field caused by operating electrical sources or the presence of ferromagnetic materials [2,30,31]. Hence, a reliable data fusion algorithm is needed to combine IMU/MARG sensor data. The effectiveness of the estimated orientation relies on the capacity to process and compensate for measurement errors [27,32].

There are many proposals to estimate orientation using IMU/MARG sensor data. Some approaches use the gyroscope data to estimate orientation [9,33] and the accelerometer and magnetometer data to correct the orientation [1,24,34]. In contrast, others use a digital motion processor (DMP) to acquire the orientation in some applications [30,35].

Human body segments can be modeled as an articulate chain of multiple body segments connected by joints. This method individually estimates the orientation of two contiguous body segments and their relative orientation. The orientation of individual body segments can be estimated by the attachment of an IMU/MARG sensor to the evaluated body segment. The relative orientation is computed by calculating the relative orientation of two adjacent body segments [34,36,37].

Different ways for representing 3D orientation have been adopted; Euler angles, Direction Cosine Matrix (DCM), and quaternions (q) are among the most common approaches. Euler angles are commonly used for orientation representation since they are relatively easy to implement. However, they are subjected to singularity conditions (e.g., gimbal lock). No singularity conditions are reported when DCM or Quaternions are used. Nonetheless, both methods entail a higher computational cost than Euler's [9].

1.1. Related works

Inertial Measurement Units (IMUs) and Magnetic Angular Rate Gravity sensors (MARGs) have been widely used in motion capturing and gait motion tracking applications. Studies for gait analysis focus on

two main aspects: 1) the estimation of kinematic and spatiotemporal parameters and 2) the tracking accuracy of the gait movement. Both aspects require the measurements of an established system. The former uses the IMU/MARG-based system to collect data from the lower limb segments to determine gait speed, stride length, stride time, step length, cadence, joints angles, peak-to-peak movements of the joints, etc. [27,38], while the latter uses the system's data recorded to analyze the body segments activity during gait [1,9,24,28,30,35].

In [27], a validation study of the accuracy of a gait analysis algorithm is presented. Two commercial IMUs (Physilog 5) were used for data collection. Data were analyzed using zero-update velocity and Kalman filtering methodology to obtain spatiotemporal gait parameters. An OptoGait system was used as the reference method for validation purposes. Linear regression studies and Bland Altman plots were used to identify correlation and suitability between the responses obtained using both methods. Based on the experimental results, the authors comment that the evaluated algorithm can estimate spatiotemporal gait parameters with a precision comparable to similar studies. However, more experiments should be performed to verify the deviations in assessing long strides. In [38] a method based on inertial sensors is presented to estimate the gait parameters of a four-segment leg model (Shanks and thighs). Inverse kinematics and a standard two-state Kalman Filter (Euler angle and gyroscope bias) were used to fuse gyroscope and accelerometer data. The system proposed by the authors allows the analysis up to 5 points simultaneously offline after a post-processing stage. For the evaluation, the angular position of the four-segment leg model in the sagittal plane, calculated from the inertial sensors (Kalman filter), was compared with data from a 3D motion capture system. Differences between both data sets were described based on the RMSE values. The accuracy of the Kalman-filtered angular position is reported to be in the range of 2–6°. The authors comment that despite the experimental results showing a good performance, small errors due to the misalignment of the sensors give rise to cumulative underestimation values. They suggest that 3D measurement of acceleration and gyroscope data and appropriate filters for data fusion, could reduce the error caused by misaligned sensors. Reference [1] presents a wearable, low-cost wireless and embedded system to simultaneously analyze trunk, pelvis, hip, knee and ankle kinematic data during gait. Complementary Filter (CF) and Kalman Filter (KF) were used to assess the system performance. Experimental results were compared with those obtained with a commercial video-based system. The Bland-Altman method was used for this purpose. The authors comment that CF and KF agree well with the results using post-processed video. Roll and pitch angles present the best results, while yaw angles seem to be affected by magnetometer distortions. In [9], a system based on inertial sensors and a data fusion algorithm is presented to provide biofeedback to user and physician practices. The developed system comprises two IMU-based portable sensing nodes, a bio-feedback generation unit, and data processing software. Body motion tracking was done by integrating angular information acquired from the sensing platform that sends data to a central unit for offline calculations. The DMP on the IMU (Invensense MPU9250) was used to acquire data from all sensors providing attitude information through a quaternion representation. The orientation accuracy of the sensor node was measured by converting the obtained quaternions into Euler angles and directly comparing them with those obtained using a Polhemus Patriot System. The authors comment that only the roll and pitch angles (X and Y axes) were measured since yaw angles (rotations around Z-axis) were strongly affected by the magnetometer field generated by the Polhemus. The experimental results show a mean error of 0.8685° and RMS of 0.9871°. In [24], an ambulatory gait analysis system based on MARG sensors is proposed. Along with this, a calibration method was introduced to avoid measurement errors of the magnetometer concerning environmental interference and inherent error. For the experimental procedure, healthy and gait-impaired patients were asked to walk through an obstacle-free corridor. Raw data from the motion sensors were collected and transmitted to a processing

unit for further analysis. A quaternion complementary filtering (CF) algorithm based on the PI control strategy was proposed to eliminate errors caused by sensor noise. The authors comment that the proposed method presents significant advantages in terms of accuracy and efficiency (3°) compared to conventional gait analysis approaches such as the traditional Kalman Filter (5°). The experimental results suggest that the proposed method by the authors is less susceptible to magnetic disturbances after the proposed calibration procedure. In [28] is evaluated the validity and reliability of Inertial Measurement Unit (IMU)-based gait analysis systems. A total of seven modules, IMU/AHRS (Invensense MPU9250), were used to measure and analyze joint angles during gait. The gradient descent algorithm was used to compute Euler angles from the gyroscope, accelerometer, and magnetometer data. Inaccurate gyroscope measurements were corrected based on the accelerometer and magnetometer data. Three healthy adult males participate in the study, which consists of a gait of 10-m. The sagittal, frontal, and transverse planes inspected the hip, knee, and ankle joints. The evaluation was performed using a camera-based system and an IMU/AHRS-based system. The differences between the RMSE values of the two systems ranged from 1.83 to 3.98°. Based on the experimental results, the authors comment that IMU-based systems can reliably replace camera-based systems for clinical analyzes of body movement and gait. In [30] a study is presented to validate the accuracy of pose estimation techniques using an optical motion capture system and a method based on MARG sensors. Three separate motions (knee flexion/extension, walking, and knee flexion/valgus/external rotations) were analyzed for the assessment. All the data obtained were computed by the software (optical motion capture method - Motiv) and the algorithm (MARG sensor-based method - EKF-based algorithm) provided by the manufacturers. The RMSE values of the angles measured using both methods were compared for validation. Based on the experimental results, the authors comment that the orientation of the MARG sensors was adequately estimated. Nonetheless, while it is true that the EKF-based method achieves a high estimation accuracy for the Roll/Pitch Euler angles (RMSE values between 1.5° to 2.92°), the yaw angle has low accuracy. It tends to drift, which could be because the magnetometer suffers from distortion and magnetic disturbance and the gyroscope suffers from drift bias. In [35], an economical and portable IMU-based system for assessing the body joint is presented. Here, a Digital Motion Processor (DMP) was used to calibrate the sensors and compute orientation by providing an integrated motion fusion output. Despite the good results, the authors suggest including information from magnetometer sensors to reduce drift and using better algorithms such as Kalman filter (KF) or Complementary filter (CF) to obtain more reliable and accurate orientation data.

This paper presents a method for the hip and lower limb 3D motion tracking based on their individual and relative orientation, either as multiple individual body segments or as an articulated body chain. The method performance was assessed by a customized Ambulatory Sensing Motion System (ASMS) consisting of seven monitoring devices. A Double-Stage Data Fusion Algorithm (algorithm-based system) for IMU/MARG-based wearable sensors was proposed to estimate the body segment orientation. Gyroscope data was used for the orientation estimation during movement and the accelerometer/magnetometer data for the orientation correction. Compensations of magnetic distortions (hard iron) and the effects of erroneous measurements due to declination/inclination magnetic disturbances (soft iron) were included. Two complementary filters were used to eliminate error measurements and to combine the responses obtained as a first approximation. A Proportional Integral controller (PI) incorporated the processed data. An approach based on quaternions was employed for the orientation estimation, a Direction Cosine Matrix quaternion-based (DCM) for estimating the relative orientation between the body segments, and Euler angles for the orientation representation. The double-stage algorithm-based system was compared with a digital motion processor (DMP) performance. RMSE values and the Bland-Altman method were used for this purpose.

2. Methodology

2.1. Ambulatory sensing motion system

The Ambulatory Sensing Motion System (ASMS), Fig. 1, consists of a modular system of seven elements: one *monitoring&computing* module (M&C), which is used both for estimating the orientation of the hip as well as for the acquisition, processing, and fusion, and sending/receiving of data of the whole system, and six *monitoring modules* (M₂₋₇), used for estimating the orientation of the lower limbs; *left and right thigh, leg and foot*.

Magnetic Angular Rate Gravity (MARG) sensors were used as a main source of information for motion tracking. Each MARG sensor is a combination of triaxial magnetometers and an Inertial Measurement Unit (IMU), which contains triaxial gyroscopes, triaxial accelerometers and a digital motion processor (DMP).

An open-source development board (*Arduino*) was used for the data interface between the M&C and M₂₋₇ modules, via Inter-Integrated Circuit serial protocol (I²C), two Multiplexers (MUX) were used to select the monitoring module of interest. The ASMS and PC communication was carried out using radio frequency modules (*Xbee*). Data acquisition and storage, motion analysis, and motion tracking were performed using the Matlab R2018a software. The components of the ambulatory Sensing Motion System are summarized in Table 1.

2.2. Estimation of the orientation

A Double-Stage Data Fusion Algorithm (algorithm-based system) was proposed, combining data from the gyroscope, accelerometer, and magnetometer sensors. The Digital Motion Processor (DMP) contained on the *Invensense* MPU was used as a reference system for validating the information. In both cases, the gyroscope and accelerometer were configured at ±250°/s and ±2g, respectively, with an output speed of 1 kHz and a digital low-pass filter (DLPF) with a bandwidth of 5 Hz (19 ms). The magnetometer was configured at ±1.3Gauss with a digital resolution of 0.92 mG. The sensors configuration is summarized in Table 1. These parameters are based on the reported values in the joint's kinematics evaluation [39–41]. The motion processing algorithms were executed at 200 Hz, to provide accurate results with low latency; no clipping was observed in the measurements.

2.2.1. Estimation of the orientation of hip and lower limbs using a Double-Stage data fusion Algorithm.

For estimating the orientation of the hip and lower limbs, either as multiple individual body segments or as an articulated body chain, a Double-Stage Data Fusion Algorithm (algorithm-based system) was proposed, Fig. 2. For the first stage, two coordinate systems were defined: a body coordinate system (σ_ω) associated with the movement of the body segment under analysis, and a reference coordinate system (σ_i), used for motion analysis as a reference frame. In the second stage, the orientation of one body segment was estimated with respect to the orientation of another contiguous segment from the spatial relationship between them. This offers great potential to be used in motion analysis and motion tracking applications of multiple body segments [24].

The body coordinate system (σ_ω) uses gyroscope data (ω_{xyz}) and its offset values ($\omega_{off_{xyz}}$) for the orientation estimation during motion, over the sampling interval (Δ_t), Eq. (1).

$$\left. \begin{aligned} \omega_{xyz} &= [g_x, g_y, g_z] \\ \omega_{off_{xyz}} &= \frac{\sum_{i=1}^{n=1000} (\omega_{xyz})_i}{n} \end{aligned} \right\} \sigma_\omega = (\omega_{xyz} - \omega_{off_{xyz}}) * \Delta_t \quad (1)$$

The reference coordinate system (σ_i) uses accelerometer ($\lambda_{a_{xyz}}$) and magnetometer data ($\lambda_{h_{xyz}}$) for the orientation correction. Two orientation correction vectors were defined for this purpose. The first one (σ_{λ_a})

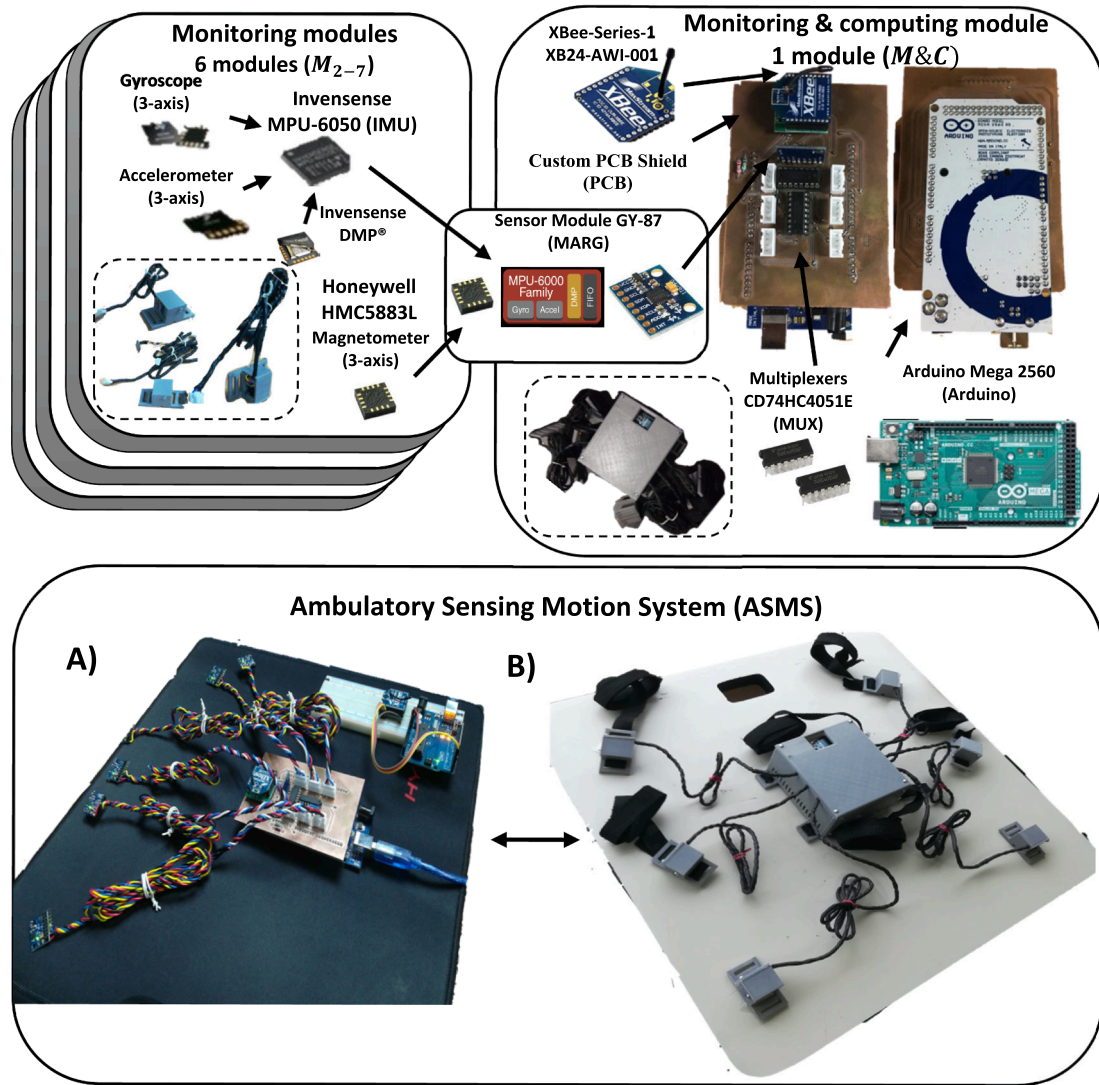


Fig. 1. Ambulatory Sensing Motion System (ASMS).

Table 1
Components of the Ambulatory Sensing Motion System (ASMS).

Module	Body segment	Function	Components	Configuration
$M\&C$	Hip	Motion tracking	Magnetic Angular Rate Gravity sensor (MARG/GY-87 module) • Triaxial magnetometers (Honeywell HMC5883L) • Inertial Measurement Unit (IMU/InvenSense MPU-6050) - Triaxial gyroscopes - Triaxial accelerometers - Digital Motion Processor (DMP) - Arduino Mega 2560 (Arduino) - Multiplexers (MUX/CD74HC4051E) Radio frequency modules (Xbee/Xbee-Series1-XB24AWI-001)	$\pm 1.3\text{Gauss}/0.92\text{mGauss}$ $1\text{ kHz} - 5\text{Hz}(19\text{ms})$ $\pm 250^\circ / \text{s}$ $\pm 2\text{g}$ 200Hz I^2C
		Interface between $M\&C$ and M_{2-7} modules Communication between ASMS and PC		
M_2	Left Thigh	Motion tracking	Magnetic Angular Rate Gravity sensor (MARG/GY-87 module) - Triaxial magnetometers (Honeywell HMC5883L) • Inertial Measurement Unit (IMU/InvenSense MPU-6050) - Triaxial gyroscopes - Triaxial accelerometers - Digital Motion Processor (DMP)	$\pm 1.3\text{Gauss}/0.92\text{mGauss}$ $1\text{kHz} - 5\text{Hz}(19\text{ms})$ $\pm 250^\circ / \text{s}$ $\pm 2\text{g}$ 200Hz
M_3	Left Leg			
M_4	Left Foot			
M_5	Right Thigh			
M_6	Right Leg			
M_7	Right Foot			

uses vector observations from gravity for Roll&Pitch orientation correction. The other one (σ_{ih}) uses vector observations of magnetic field measurements for Yaw orientation correction.

The orientation correction vector (σ_{ia}) was computed as the vectorial product between inertial (\vec{v}) and local gravity vector (\vec{v}), Eq. (2).

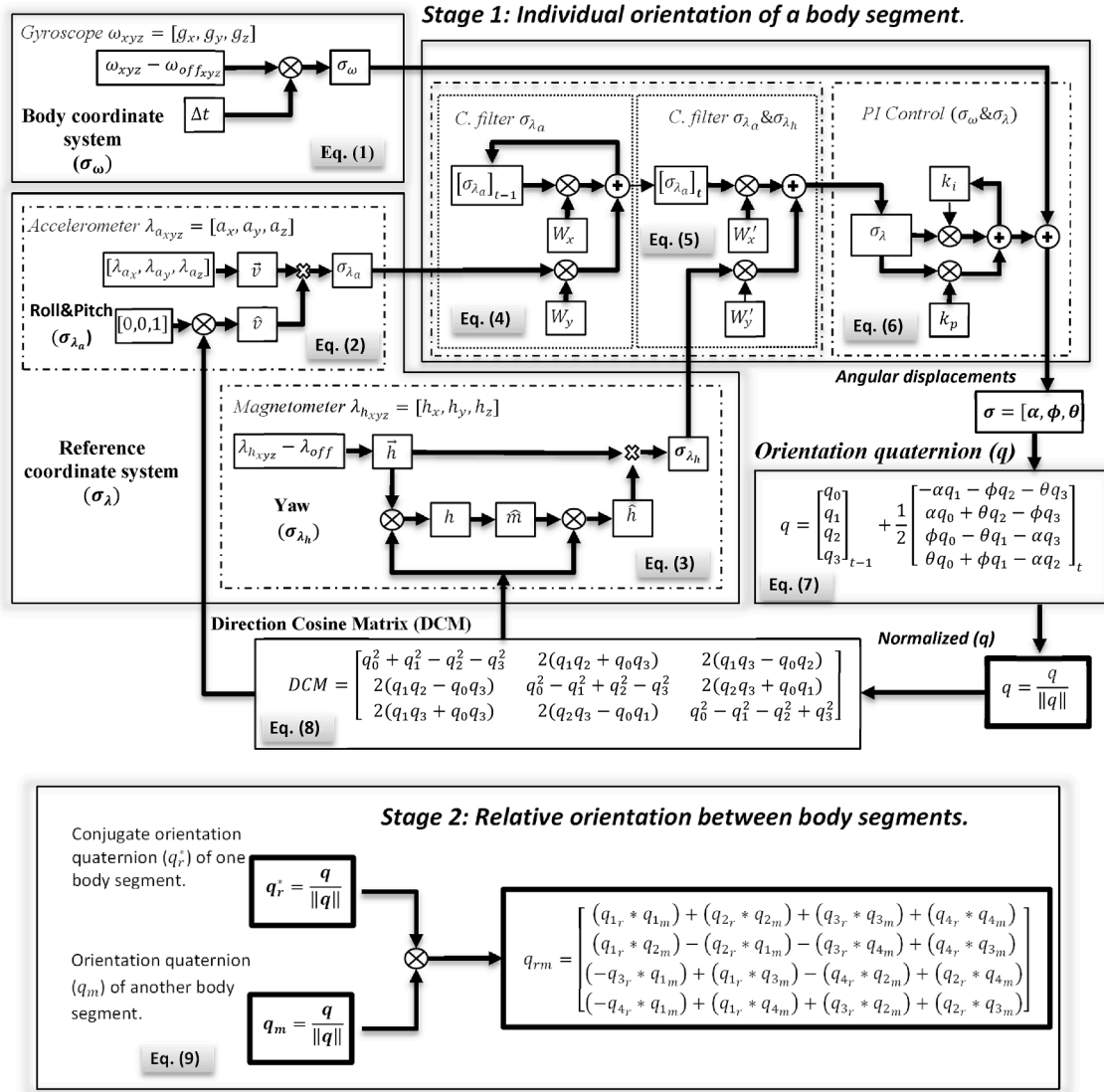


Fig. 2. Double-Stage Data Fusion Algorithm: Stage 1: Individual orientation of a body segment; the same process is applied for estimating both, the orientation of the hip, and the orientation of the lower limbs, separately. Stage 2: Relative orientation between body segments (q_{rm}); orientation of one body segment (q_r) to another (q_m).

$$\left. \begin{aligned} \lambda_{a_{xyz}} &= [a_x, a_y, a_z] \\ \vec{v} &= \frac{\lambda_{a_{xyz}}}{\|\lambda_{a_{xyz}}\|} \\ \hat{v} &= [0, 0, 1] * DCM \end{aligned} \right\} \sigma_{\lambda_a} = \vec{v} \times \hat{v} \quad (2)$$

The orientation correction vector (σ_{λ_h}) was estimated from the cross product between magnetic flux (\vec{h}) and directional (\hat{h}) vectors, Eq. (3). The first one uses magnetometer data ($\lambda_{h_{xyz}}$) and its offset values ($\lambda_{h_{off}}$) for compensating magnetic distortions (hard iron). The second one was computed by relating (\vec{h}) to its relative orientation, thus, defining the magnetic field direction (h). To avoid the effects of declination and inclination magnetic disturbances (soft iron), the magnetic field direction (h) was denoted in terms of the horizontal and vertical axes of the reference system defining the directional vector (\hat{m}) which is related to its relative orientation to obtain the corrected directional vector (\hat{h}).

$$\left. \begin{aligned} \lambda_{h_{xyz}} &= [h_x, h_y, h_z] \\ \lambda_{h_{off}} &= \frac{\max(\lambda_h) - \min(\lambda_h)}{2} \\ h &= \vec{h} * DCM \\ \hat{m} &= [\sqrt{h_x^2 + h_y^2}, 0, h_z] \end{aligned} \right\} \vec{h} = \left(\frac{\lambda_{h_{xyz}}}{\|\lambda_{h_{xyz}}\|} \right) - \lambda_{h_{off}} \quad (3)$$

$$\left. \begin{aligned} h &= \vec{h} * DCM \\ \hat{m} &= [\sqrt{h_x^2 + h_y^2}, 0, h_z] \end{aligned} \right\} \hat{h} = \hat{m} * DCM$$

Two complementary filters were used; (C. filter σ_{λ_a}) to eliminate error measurements from σ_{λ_a} , Eq. (4), and (C. filter σ_{λ_a} & σ_{λ_h}) for defining the reference coordinate system (σ_λ), Eq. (5).

$$[\sigma_{\lambda_a}]_t = W_x[\sigma_{\lambda_a}]_{t-1} + W_y[\sigma_{\lambda_a}] \quad (4)$$

$$\sigma_\lambda = W_x'[\sigma_{\lambda_a}]_t + W_y'[\sigma_{\lambda_h}] \quad (5)$$

Heuristics were used for weighted values of W_x, W_y, W_x', W_y' .

A PI controller (σ_ω & σ_λ) was used for gradually incorporate data between coordinate systems: σ_ω and σ_λ , as angular displacements (σ), Eq. (6).

$$\sigma = \sigma_\omega + \left[k_p(\sigma_\lambda) + k_i \int_0^t f(\sigma_\lambda) \right] = [\alpha, \phi, \theta] \quad (6)$$

The good gain method [42,43] was used for k_p & k_i values.

The angular displacements (σ) were used to estimate the spatial relationship between coordinate systems using quaternions (q), normalized quaternions to guarantee orthogonality and normativity of the estimated body segment orientation, and a Direction Cosine Matrix quaternion-based (DCM) for defining the new coordinate systems relative orientation, Eq. (7) and Eq. (8). The same process was applied for estimating both, the orientation of the hip, and the orientation of the lower limbs, separately.

$$q = q_{t-1} + \int_0^t q(dt) = q_{t-1} \otimes q_t = \begin{bmatrix} q_0 \\ q_1 \\ q_2 \\ q_3 \end{bmatrix}_{t-1} + \frac{1}{2} \begin{bmatrix} -\alpha q_1 - \phi q_2 - \theta q_3 \\ \alpha q_0 + \theta q_2 - \phi q_3 \\ \phi q_0 - \theta q_1 - \alpha q_3 \\ \theta q_0 + \phi q_1 - \alpha q_2 \end{bmatrix}_t \quad (7)$$

$$q = \frac{q}{\|q\|}$$

$$DCM = (q_0^2 - q_1^2 - q_2^2 - q_3^2) \begin{bmatrix} 1 & 0 & 0 \\ 0 & 1 & 0 \\ 0 & 0 & 1 \end{bmatrix} + 2q_1q_2' + 2q_0 \begin{bmatrix} 0 & -q_3 & q_2 \\ q_3 & 0 & -q_1 \\ -q_2 & q_1 & 0 \end{bmatrix} \quad (8)$$

$$DCM = \begin{bmatrix} q_0^2 + q_1^2 - q_2^2 - q_3^2 & 2(q_1q_2 + q_0q_3) & 2(q_1q_3 - q_0q_2) \\ 2(q_1q_2 - q_0q_3) & q_0^2 - q_1^2 + q_2^2 - q_3^2 & 2(q_2q_3 + q_0q_1) \\ 2(q_1q_3 + q_0q_3) & 2(q_2q_3 - q_0q_1) & q_0^2 - q_1^2 - q_2^2 + q_3^2 \end{bmatrix}$$

Once hip and lower limbs orientation was estimated separately, the orientation of one body segment (q_r) to another (q_m) is computed as shown in Eq. (9).

$$q_{rm} = q_r^* \otimes q_m \quad (9)$$

$$q_{rm} = \begin{bmatrix} (q_{1r}^* q_{1m}) + (q_{2r}^* q_{2m}) + (q_{3r}^* q_{3m}) + (q_{4r}^* q_{4m}) \\ (q_{1r}^* q_{2m}) - (q_{2r}^* q_{1m}) - (q_{3r}^* q_{4m}) + (q_{4r}^* q_{3m}) \\ (-q_{3r}^* q_{1m}) + (q_{1r}^* q_{3m}) - (q_{4r}^* q_{2m}) + (q_{2r}^* q_{4m}) \\ (-q_{4r}^* q_{1m}) + (q_{1r}^* q_{4m}) + (q_{3r}^* q_{2m}) + (q_{2r}^* q_{3m}) \end{bmatrix}$$

Where q_r^* is the conjugate orientation quaternion of the reference body segment and q_m the orientation quaternion of another body segment.

The same process is applied for estimating the relative orientation between the body segments. Each body segment is differentiated by subscripts labeled according to the module location (see 2.3.1 Location of the modules: monitoring&computing, and monitoring modules).

2.2.2. Orientation estimation of the hip and lower limbs using a Digital motion Processor

Two stages were defined for the orientation estimation using a Digital Motion Processor (DMP). In the first stage, the DMP was used to obtain the orientation quaternion (q) of the hip and the lower limbs independently. In the second stage, the information of each body segment, obtained from the DMP, was used to determine the orientation of one segment concerning the orientation of another (q'_{rm}), as described in equation (9).

2.3. Study procedure

2.3.1. Location of the modules: monitoring&computing, and monitoring modules

Seven modules were used to track the movement of the hip (M1-M&C), and lower limbs (M2-M7) during their movement, Fig. 3a. M1 –M&C was placed in the pelvis, aligned on the sagittal plane and the medial line of the body, and in transverse and coronal planes with the iliac crest. M2-M7 were divided into two sections; left & right, and three subsections; thigh, leg, and foot. Modules M2&M5 were located at the anterior portion of the thigh, centered on sagittal plane and the medial line of the leg, and the coronal plane in the middle distance between the

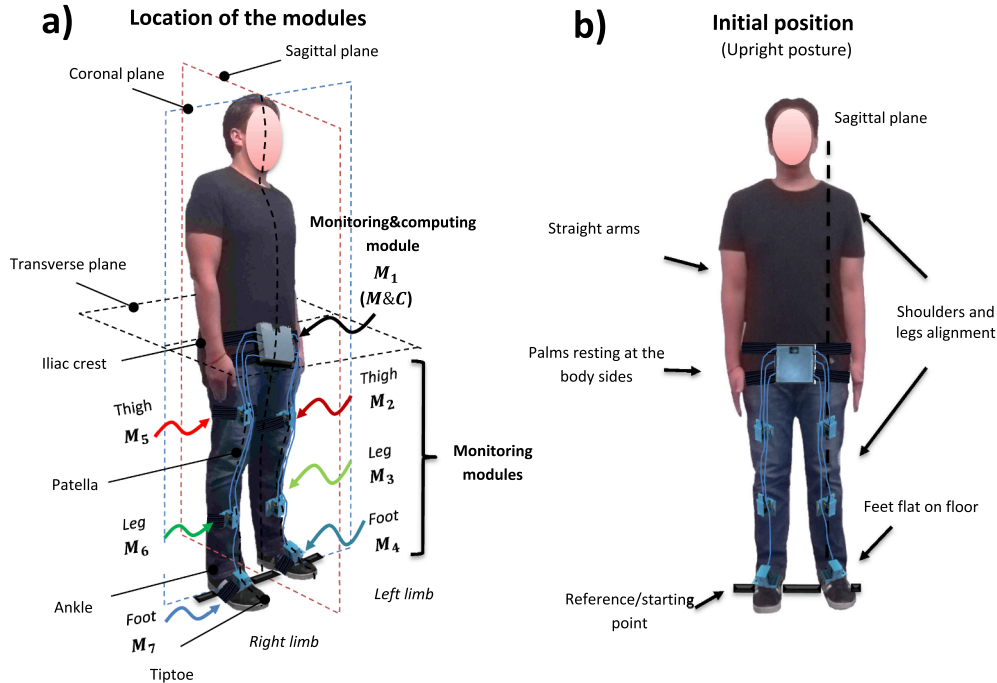


Fig. 3. Location of the modules; monitoring&computing module ($M_1 - M\&C$) y monitoring modules ($M_2 - M_7$), and initial position for the experimental procedure.

iliac crest and the patella; *M3&M6* on the anterior portion of the leg, centered on sagittal plane and the midline of the leg, and the coronal plane at the median distance between the patella and the ankle; *M4&M7* on the front face of the foot (metatarsal), centered on sagittal plane and the midline of the foot, and in the transverse plane in the middle distance between the ankle and the ball of the foot. Elastic bands were used for attaching the modules to the body segments.

2.3.2. Participants

Six women and six men, 25–35 years and 160–185 cm average height, were recruited for the study. Subjects without apparent neuromuscular problems, injuries, or recent surgeries were admitted as inclusion criteria. The testing was explained to the participants before and during its development, an informed consent was signed for each of the participants. The experimental tests were performed with the consent of the Instituto Politécnico Nacional Ethics committee.

2.3.3. Initial position

The initial position was upright posture, Fig. 3b, straight arms, palms resting at the body sides, shoulders and legs alignment on the sagittal plane, and feet flat on the floor placed over a horizontal line marked on the base (floor) used as a reference/starting point.

2.4. Evaluation of the algorithm-based system

This process consisted of measuring and recording the sensors' data to discard error measurements before the evaluation. Wearing the sensors modules', the participants were asked to adopt the initial position, placing both feet on the horizontal reference line and staying in that position during the calibration procedure. Then participants were asked to gait in a straight line, at a steady speed, until completing ten steps (5 steps for each leg), starting with the right foot, and ending the movement with the alignment of both feet (same as on the initial position). Two audible marks were used to indicate the beginning/ending of the test to participants. The test was realized on a flat walkaway of 10 m with no obstacles.

The algorithm-based system and the digital motion processor (DMP)

were used for simultaneously recording the hip and lower limbs' Range of Motion (RoM). The recorded data was used for performing a 2D&3D motion representation of the described trajectory by the hip and lower limbs, Fig. 4.

For the 2D representation, a conversion from the orientation quaternion (q) to Euler angles was performed, as shown in equation (10).

$$\begin{bmatrix} \alpha \\ \phi \\ \theta \end{bmatrix} = \begin{bmatrix} \arctan \frac{2(q_0q_1 + q_2q_3)}{1 - 2(q_1^2 + q_2^2)} \\ \arcsin(2(q_0q_2 - q_3q_1)) \\ \arctan \frac{2(q_0q_3 + q_1q_2)}{1 - 2(q_2^2 + q_3^2)} \end{bmatrix} \quad (10)$$

Twenty-one plots were arrayed into seven sets of three graphs within the same figure. The first set was used to represent the angular displacements (α, ϕ, θ) described by the hip (*M1–M&C*) around each of the reference coordinate axes (X, Y, Z). The following three sets were used for the angular displacements of the lower left limb: left thigh (*M2*), left leg (*M3*), and left foot (*M4*). Finally, the last three sets were used for the lower right limb: right thigh (*M5*), right leg (*M6*), and right foot (*M7*).

For the 3D motion representation, a 3D arbitrary point with coordinates $[0, 0, -1]$ was defined as an initial stage (t_0), the DCM quaternion-based equation (8), was used for defining new coordinates $[x, y, z]$ of this point, equation (11).

$$[x, y, z] = [DCM^*[0, 0, -1]]_{t_0}^n \quad (11)$$

Where n is represents total number of samples.

Considering that different methods were used for recording data, a qualitative/quantitative analysis was performed to identify drift and noise levels, and to verify the agreement between the algorithm-based system and DMP responses, the latter based on the Bland-Altman method [27,44–46]. For this purpose, the X, Y, and Z values of each data set were compared, in search of systematic errors and possible outliers, based on the mean between the results obtained of both methods (mean of algorithm & DMP) and, the average differences regarding its limits of agreement (Differences), Fig. 5 and Fig. 6.

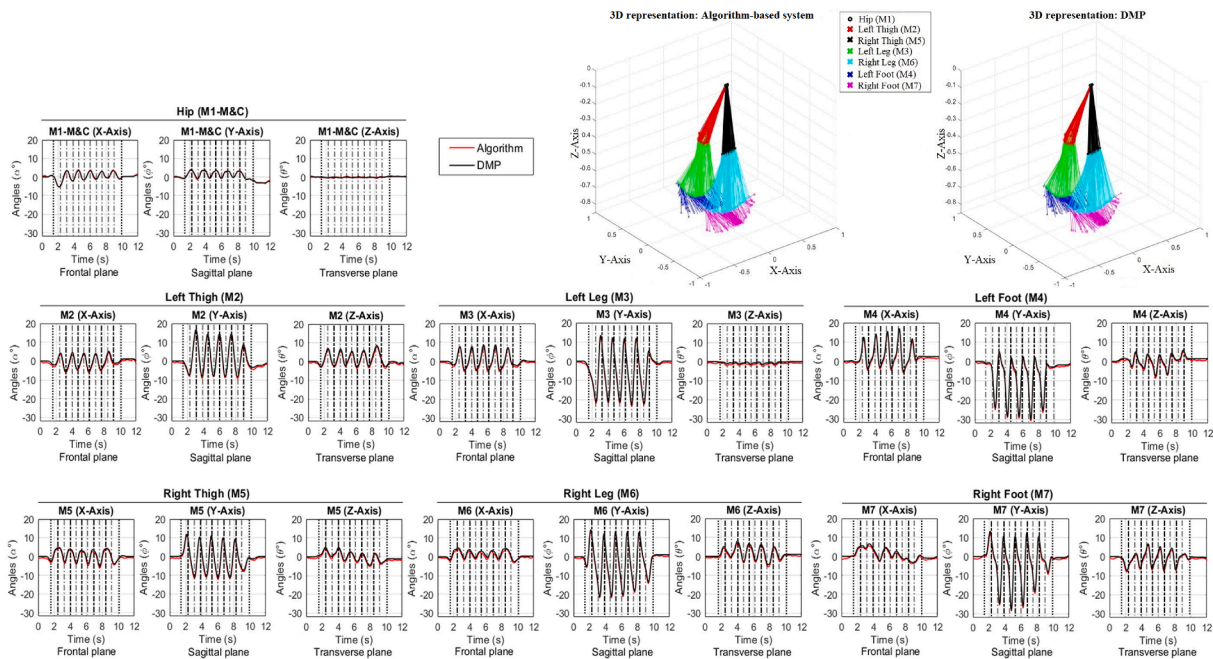


Fig. 4. 2D and 3D representation of the trajectory described by the evaluated body segments: angular displacements (α, ϕ, θ) described by the hip (*M1-M & C*), and the segments of the lower extremities, left and right; thigh (*M2&M5*), leg (*M3&M6*), and foot (*M4&M7*), with respect to each of the coordinate axes of evaluation (X, Y, Z), during the execution of the gait movement, using the proposed algorithm-based system and the DMP.

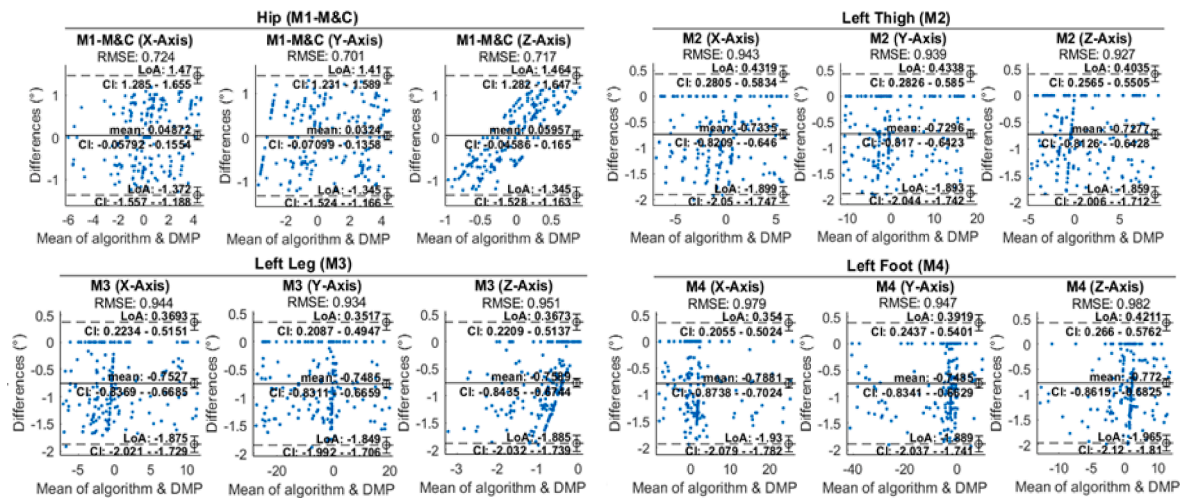


Fig. 5. BlandAltman (Agreement between Algorithm-based system&DMP): Comparison of the angular displacements (α, ϕ, θ), described by the hip (M1-M&C) and the segments of the left; thigh (M2), leg (M3) and foot (M4), with respect to each of the evaluation coordinate axes (X, Y, Z).

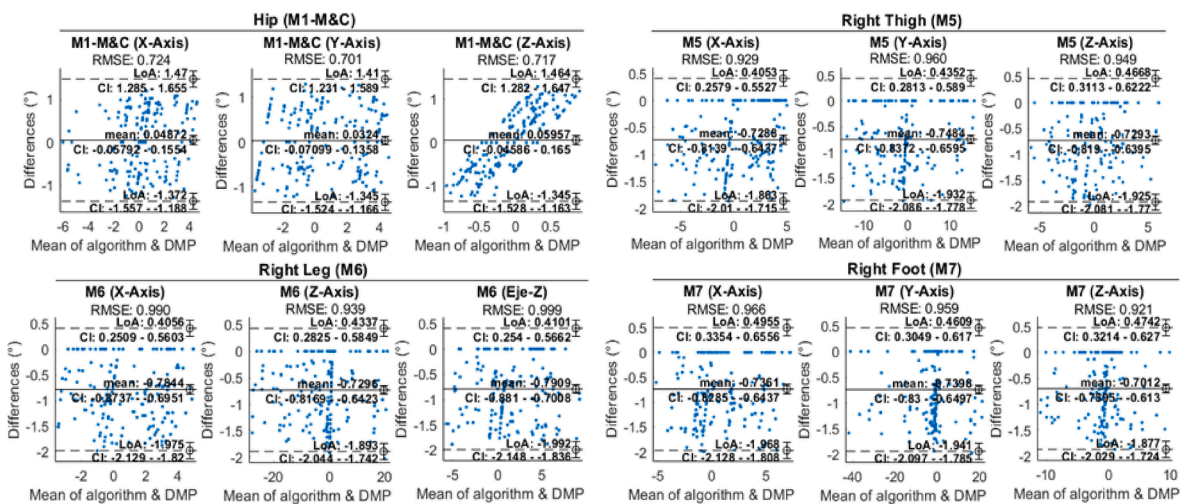


Fig. 6. BlandAltman (Agreement between Algorithm-based system&DMP): Comparison of the angular displacements (α, ϕ, θ), described by the hip (M1-M&C) and the segments of the right; thigh (M5), leg (M6) and foot (M7), with respect to each of the evaluation coordinate axes (X, Y, Z).

3. Results

For its analysis, the 2D representation of the trajectory described by the hip and lower limbs, Fig. 4, was divided into thirteen segments and four stages. The first segment corresponds to the first stage (stationary phase/Initial position). The following ten segments - second stage (Gait movement), in which ten steps are performed (5 steps for each leg). The twelfth segment - third stage (alignment phase), in which the rear limb gradually advances until it is aligned with its counterpart. In the thirteenth segment - fourth stage (stationary phase/Initial position), both limbs are aligned, and the body adopts the initial position.

The angular displacements in the X axis are abduction-adduction/inversion-eversion movements (rotation axis; anteroposterior, the plane of execution; frontal), Y axis, flexion-extension/plantarflexion-dorsi-flexion movements (rotation axis; transverse, the plane of execution -sagittal), and Z axis, internal-external/medial-lateral rotations in its axis (rotation axis; vertical, the plane of execution; transverse).

Regarding the Bland Altman representation (agreement between methods), Fig. 5 and Fig. 6, the data was plotted as a function of the responses obtained of both methods (mean of algorithm & DMP), the DMP as our reference method. The average differences between the responses of the algorithm-based system and DMP (Differences) suggest

the absence of systematic errors or significant outliers. This is based on the symmetry of the distribution of data points regarding the bias and considering that these points are within the limits of agreement (LoA). The upper and lower limits of agreement (LoA) represent the maximum variation range between methods. These ranges were defined with a 95% confidence interval.

4. Discussion

Many proposals IMU/MARG sensors-based, including commercial systems, have been reported, some of them are oriented to the assessment of specific activities, providing processed information [33,47,48], and in some other cases, the information is recorded in SD memory or transmitted to a PC for processing [49-51]. This supposes a limitation for motion tracking unless an external source for data post-processing is available, especially in applications oriented to ambulatory motion tracking, either during the assessment of multiple individual body segments or as an articulated body chain, such as the case of gait motion. Most of the proposed methods in the literature are centered on the orientation estimation of the body segments individually, which could be sufficient for analyzing specific applications such as evaluating the individual lower limbs [9,30] and gait parameters [29]. Nonetheless,

estimating the relative orientation between the body segments could offer an advantage in applications oriented to motion tracking and motion analysis of multiple body segments [24]. In both cases, a data fusion algorithm is needed for combining IMU/MARG sensor data to be used in motion-tracking applications [35,38]. In this regard, many proposals, for combining sensor data demonstrated good performance in their application have been presented by [1,9,24,28,30,38]. Deviation problems [27], small errors due to misalignment of the sensors that rise to cumulative underestimation values [38], noise measurements, drift, and magnetometer distortions [1,9,24,30], have been reported.

Concerning this work IMU/MARG sensor-based, Ambulatory Sensing Motion System (ASMS) Fig. 1, and Table 1, in combination with a Double-Stage Data Fusion Algorithm (algorithm-based system) Fig. 2, is presented, which provides not only the processed data during the assessment but also allows to store and transmit raw data to a PC for post-processing purposes if necessary. The proposed method allows 3D motion tracking of the hip and lower limbs movement (7 segments; hip and the lower body segments, left and right thigh, leg, and foot), either as multiple individual body segments or as an articulated body chain, allowing it to be used in motion tracking and motion analysis of multiple body segments. A double-stage complementary filter (CF) and PI control, including compensations of magnetic distortions, was used to combine IMU/MARG sensor data. Experimental results were compared with those obtained using a Digital Motion Processor (DMP). In [35] it was demonstrated that the DMP could provide reliable and accurate orientation data, especially if magnetic distortion compensations along with a data fusion algorithm such as the KF or CF is included.

The experimental results of this work, Fig. 4 shows that both responses, algorithm-based system and DMP, are close to each other; from this, the hypothesis is that both methods allow estimating the orientation with similar performance. It can be observed that the initial and final positions of the trajectory described by the body segments are close to each other. This behavior is expected, especially considering the initial position starts from the idle stay while the final one ends in the same body position after the gait evaluation. These observations suggest no significant drift values, especially considering that no amplitude changes that denote this phenomenon in addition to the initial and final position. Besides, there is no evidence of noise levels that suggest that the information could be corrupted. This is demonstrated by considering that the integration of erroneous measurements during the orientation estimation will cause an accumulation of drift over time [9]. This can also be seen in the 3D reconstruction of the trajectory described by the body segments, since the estimation of the orientation is concerning another body segment. If the measurements drifted, the 3D trajectory reconstruction would show an offset between the segments describing the movement performed on different planes/spaces [27]. Furthermore, no abrupt changes in the trajectory described were observed, e.g., from 90° to -90° , even when it is based on the representation of the angular displacements. This could be because the orientation estimation was performed on a quaternion-based approach, which allows the formation of a non-singular representation [9].

The Bland Altman analysis Fig. 5 and Fig. 6 showed that the algorithm-based system is neither underestimated nor overestimated. Concerning the DMP, both systems' responses are within the ranges established by the limits of agreement (LoA) without exceeding the acceptable difference [27,44,45]. The 0.7° RMSE value (M1) and 1° RMSE value (M2-M7) indicated that the algorithm-based system competes with similar proposals [1,9,24] and even with some visual-based systems [28,30,38]. These results suggest that the proposed algorithm-based system is suitable to the DMP.

4.1. Limitations of the proposed method and future work

In contrast to video-based systems, the proposed method does not need specialized personnel or a controlled evaluation environment for data capture; it is not susceptible to background conditions or occlusion

problems [18,19]. Nonetheless, further research is required to compare the proposal performance concerning a video-based system to assess the feasibility of its use in clinical settings. In this regard, the performance should be evaluated with healthy subjects and with mobility conditions to determine its usefulness for healthcare and rehabilitation applications. Numerous evaluations report interference due to magnetic disturbances, even in controlled environments, when IMU/MARG sensors are used [1,9,30,35]. To overcome this issue, compensations for magnetic distortions (hard iron) and the effects of erroneous measurements due to declination/inclination magnetic disturbances (soft iron) were included in the present proposal. Although no variations due to magnetic disturbances were observed, additional tests must be done to evaluate its performance in different settings, including outdoor environmental magnetic perturbances and other motion conditions. The proposed algorithm-based system presents similar results to a commercial Digital Motion Processor (DMP), except that it has a slower response than the DMP, which could be attributed to the parameters of the Proportional Integral controller (PI) used to integrate the orientation. In that sense, additional tests are required to define the ideal parameters for different applications.

4.2. Contributions

The proposed method allows 3D motion tracking of the hip and lower limbs movement (7 segments; hip and the lower body segments, left and right thigh, leg, and foot), either as multiple individual body segments or as an articulated body chain; one body segment with respect to another contiguous segment, providing information both during the assessment without the necessity of a post-processing stage, and for its posterior analysis. This feature presents an advantage compared with proposals that require a post-processing stage to analyze data, such as in the case of [9,24,38]. The proposed method offers a great potential to be used in ambulatory motion analysis and motion tracking with applications in different environments.

The proposed algorithm-based system presents similar results to a commercial Digital Motion Processor (DMP). The experimental results indicated 0.7° RMSE (M1, Hip) and 1° RMSE (M2-MT, left and right thigh, leg, and foot) with mean values lower than 1° when comparing the responses of both methods, no singularity conditions or significant levels of noise or drift were reported, which are comparable with those reported in [1,9,24,28,30,38]. Besides, the Double-Stage Data Fusion Algorithm proposed here is not limited to a specific system; it can be applied to different devices based on IMU/MARG sensors.

The 2D and 3D representations showed their application in motion tracking of the lower limbs during motion gait; this presents valuable information to both the user and the evaluator for visualizing and interpreting how the human motor activity was executed. The results demonstrate the feasibility of using the proposed algorithm-based system for orientation estimation of different body segments with applications in medical telerehabilitation.

5. Conclusions

This manuscript presented a method for tracking the 3D movement of the hip and lower limbs based on orientation estimation using a Double-Stage Data Fusion Algorithm for IMU/MARG sensor-based monitoring devices. A customized ambulatory sensing motion system, consisting of seven monitoring devices, was implemented for this application.

The combination of gyroscope, accelerometer, and magnetometer sensor data presents a feasible solution for estimating the 3D orientation of multiple body segments. The double state of complementary filters for eliminating measurement errors and a Proportional Integral controller to incorporate sensor data gradually allowed the proposed algorithm-based system to compete with a commercial Digital Motion Processor (DMP) with similar performance. No singularity conditions or

significant noise or drift errors were reported.

The experimental results show that the proposed method can be used for 3D human motion tracking of multiple body segments, individually or as an articulated body chain, providing information both during the assessment, without the need of a post-processing stage, and for its posterior analysis. Besides, the proposed method suits different IMU/MARG sensor-based wearable sensors.

Declaration of Competing Interest

The authors declare that they have no known competing financial interests or personal relationships that could have appeared to influence the work reported in this paper.

Data availability

Data will be made available on request.

Acknowledgments

To the Instituto Politécnico Nacional (IPN) for funding this research, Research project SIP: 20230190 and 20231622.

The authors also thank the support of M. Sc. Muñoz López Esmeralda Ivonne.

Funding

Instituto Politécnico Nacional - Research project SIP: 20230190 and 20231622.

Ethical approval

The experimental tests were performed with the consent of the Instituto Politécnico Nacional Ethics committee.

References

- [1] T.M. Santos, M.F. Barroso, R.A. Ricco, E.G. Nepomuceno, É.L. Alvarenga, Á.C. Penoni, A.F.J.M. Santos, A low-cost wireless system of inertial sensors to postural analysis during human movement, 148 (2019) 106933.
- [2] S. Qiu, Z. Wang, H. Zhao, K. Qin, Z. Li, H.J.I.F. Hu, Inertial/magnetic sensors based pedestrian dead reckoning by means of multi-sensor fusion, 39 (2018) 108–119.
- [3] K. Cahill-Rowley, J.J.J.o.b. Rose, Temporal-spatial reach parameters derived from inertial sensors: comparison to 3D marker-based motion capture, 52 (2017) 11–16.
- [4] R. Ferber, S.T. Osis, J.L. Hicks, S.L.J.J.o.b. Delp, Gait biomechanics in the era of data science, 49 (2016) 3759–3761.
- [5] R. Baker, A. Esquenazi, M.G. Benedetti, K.J.E.J.P.R.M. Desloovere, Gait analysis: clinical facts, 52 (2016) 560–574.
- [6] K. Feng, J. Li, X. Zhang, C. Shen, Y. Bi, T. Zheng, J. Liu, Correction: a new quaternion-based kalman filter for real-time attitude estimation using the two-step geometrically-intuitive correction algorithm. *Sensors* 17 (2017), 2146. *Sensors* 17 (2017) 2530.
- [7] P.K. Yoon, S. Zihajehzadeh, B.-S. Kang, E.J. Park, Robust biomechanical model-based 3-D indoor localization and tracking method using UWB and IMU, *IEEE Sens. J.* 17 (2017) 1084–1096.
- [8] C.W. Kang, H.J. Kim, C.G. Park, A human motion tracking algorithm using adaptive EKF based on Markov chain, *IEEE Sens. J.* 16 (2016) 8953–8962.
- [9] P. Buonocunto, A. Giantomassi, M. Marinoni, D. Calvaresi, G.J.A.T.o.C.-P.S. Buttazzo, A limb tracking platform for tele-rehabilitation, 2 (2018) 1–23.
- [10] M. Amboni, L. Iuppariello, A. Iavarone, A. Fasano, R. Palladino, R. Rucco, M. Picillo, I. Lista, P. Varriale, C. Vitale, Step length predicts executive dysfunction in Parkinson's disease: a 3-year prospective study, *J. Neurol.* 265 (2018) 2211–2220.
- [11] P. Sorrentino, A. Barbato, L. Del Gaudio, R. Rucco, P. Varriale, M. Sibilio, P. Strazzullo, G. Sorrentino, V. Agosti, Impaired gait kinematics in type 1 Gaucher's Disease, *J. Parkinsons Dis.* 6 (2016) 191–195.
- [12] M. Pau, G. Bernardelli, B. Leban, M. Porta, V. Putzu, D. Viale, G. Asoni, D. Riccio, S. Cerfoglio, M.J.E. Galli, Age-associated changes on gait smoothness in the third and the fourth age, 12 (2023) 637.
- [13] C.-Y. Chiang, K.-H. Chen, K.-C. Liu, S.-J.-P. Hsu, C.-T. Chan, Data collection and analysis using wearable sensors for monitoring knee range of motion after total knee arthroplasty, *Sensors* 17 (2017) 418.
- [14] S. Bao, S. Yin, H. Chen, W. Chen, A wearable multimode system with soft sensors for lower limb activity evaluation and rehabilitation, in: 2018 IEEE International Instrumentation and Measurement Technology Conference (I2MTC), IEEE, 2018, pp. 1–6.
- [15] Y. Ma, K. Mithraratne, N.C. Wilson, X. Wang, Y. Ma, Y.J.S. Zhang, The validity and reliability of a kinect v2-based gait analysis system for children with cerebral palsy, 19 (2019) 1660.
- [16] Y. Ma, B. Sheng, R. Hart, Y. Zhang, The validity of a dual Azure Kinect-based motion capture system for gait analysis: a preliminary study, in: 2020 Asia-Pacific Signal and Information Processing Association Annual Summit and Conference (APSIPA ASC), IEEE, 2020, pp. 1201–1206.
- [17] G. Nagymáté, R.M.J.P.o. Kiss, Affordable gait analysis using augmented reality markers, 14 (2019) e0212319.
- [18] M. Zago, C. Sforza, I. Pacifici, V. Cimolin, F. Camerota, C. Celletti, C. Condoluci, M. F. De Pandis, M.J.J.o.E. Galli, Kinesiology, Gait evaluation using inertial measurement units in subjects with Parkinson's disease, 42 (2018) 44–48.
- [19] X. Xu, R.W. McGorry, L.-S. Chou, J.-h. Lin, C.-c.J.G. Chang, posture, Accuracy of the Microsoft Kinect™ for measuring gait parameters during treadmill walking, 42 (2015) 145–151.
- [20] K. Suri, R.J.C. Gupta, E. Engineering, Continuous sign language recognition from wearable IMUs using deep capsule networks and game theory, 78 (2019) 493–503.
- [21] S. Beausoleil, L. Miramand, K.J.G. Turcot, Posture, Evolution of gait parameters in individuals with a lower-limb amputation during a six-minute walk test, 72 (2019) 40–45.
- [22] G. Li, T. Liu, J.J.I.S.J. Yi, Wearable sensor system for detecting gait parameters of abnormal gaits: a feasibility study, 18 (2018) 4234–4241.
- [23] J.P. Amaro, S. Patrão, A survey of sensor fusion algorithms for sport and health monitoring applications, in: IECON 2016-42nd Annual Conference of the IEEE Industrial Electronics Society, IEEE, 2016, pp. 5171–5176.
- [24] S. Qiu, Z. Wang, H. Zhao, L. Liu, J. Li, Y. Jiang, G.J.I.S.J. Fortino, Body sensor network-based robust gait analysis: toward clinical and at home use, 19 (2018) 8393–8401.
- [25] P.A.C. Widagdo, H.-H. Lee, C.-H. Kuo, Limb motion tracking with inertial measurement units, in: 2017 IEEE International Conference on Systems, Man, and Cybernetics (SMC), IEEE, 2017, pp. 582–587.
- [26] S. Qiu, L. Liu, H. Zhao, Z. Wang, Y.J.M. Jiang, MEMS inertial sensors based gait analysis for rehabilitation assessment via multi-sensor fusion, 9 (2018) 442.
- [27] L. Zhou, C. Tunca, E. Fischer, C.M. Brahm, C. Ersoy, U. Granacher, B. Arrnrich, Validation of an IMU gait analysis algorithm for gait monitoring in daily life situations, in: 2020 42nd Annual International Conference of the IEEE Engineering in Medicine & Biology Society (EMBC), IEEE, 2020, pp. 4229–4232.
- [28] Y.-S. Cho, S.-H. Jang, J.-S. Cho, M.-J. Kim, H.D. Lee, S.Y. Lee, S.-B.J.A.o.r.m. Moon, Evaluation of validity and reliability of inertial measurement unit-based gait analysis systems, 42 (2018) 872–883.
- [29] K. Li, C. Zhou, Estimation of gait parameters based on motion sensor data, *BIODEVICES* (2020) 129–135.
- [30] Y. Igarashi, A. Komatsu, T. Iwami, H. Tsukamoto, Y. Shimada, Comparison of MARG sensor results for different mounting positions and physiques for accurate knee joint motion measurement, in: 2019 4th Asia-Pacific Conference on Intelligent Robot Systems (ACIRS), IEEE, 2019, pp. 49–52.
- [31] P. Chinmilli, S. Redkar, W. Zhang, T.J.I.R.A.J. Sugar, A review on wearable inertial tracking based human gait analysis and control strategies of lower-limb exoskeletons, 3 (2017) 00080.
- [32] P. Pierleoni, A. Belli, L. Palma, M. Mercuri, F. Verdini, S. Fioretti, S. Madgwick, F. Pintì, Validation of a gait analysis algorithm for wearable sensors, in: 2019 International Conference on Sensing and Instrumentation in IoT Era (ISSI), IEEE, 2019, pp. 1–6.
- [33] M. Guidolin, R.A.B. Petrea, O. Roberto, M. Reggiani, E. Menegatti, L. Tagliapietra, On the accuracy of imus for human motion tracking: a comparative evaluation, in: 2021 IEEE International Conference on Mechatronics (ICM), IEEE, 2021, pp. 1–6.
- [34] S. Qiu, Z. Wang, H. Zhao, L. Liu, J. Wang, J. Li, Gait Analysis for Physical Rehabilitation via Body-Worn Sensors and Multi-information Fusion, *Advances in Body Area Networks I*, Springer, 2019, pp. 139–148.
- [35] Y.C.S.Z.C. Ong, S.Y. Khoo, S. Noroozi, Development of an economic wireless human motion analysis device for quantitative assessment of human body joint, *Measurement* 115 (2018) 306–315.
- [36] J.A. Barraza Madrigal, J.C. Negrete, R.M. Guerrero, L.A.C. Rodríguez, H.J.B. Sossa, B. Engineering, 3D motion tracking of the shoulder joint with respect to the thorax using MARG, *Sensors Data Fusion Algorithm* 40 (2020) 1205–1224.
- [37] J.A. Barraza Madrigal, E. Cardiel, P. Rogeli, L.L. Salas, R.M. Guerrero, Evaluation of suitability of a micro-processing unit of motion analysis for upper limb tracking, *Med. Eng. Phys.* 38 (2016) 793–800.
- [38] K. Bötzel, A. Olivares, J.P. Cunha, J.M.G. Sáez, R. Weiss, A.J.J.o.b. Plate, Quantification of gait parameters with inertial sensors and inverse kinematics, 72 (2018) 207–214.
- [39] Y.-C. Lai, C.-C. Chang, C.-M. Tsai, S.-C. Huang, K.-W. Chiang, A knowledge-based step length estimation method based on fuzzy logic and multi-sensor fusion algorithms for a pedestrian dead reckoning system, *ISPRS Int. J. Geo Inf.* 5 (2016) 70.
- [40] S. Tadano, R. Takeda, H. Miyagawa, Three dimensional gait analysis using wearable acceleration and gyro sensors based on quaternion calculations, *Sensors* 13 (2013) 9321–9343.
- [41] Z. Ercan, V. Sezer, H. Heceoglu, C. Dikilitas, M. Gokasan, A. Mugan, S. Bogosyan, Multi-sensor data fusion of DCM based orientation estimation for land vehicles, in: 2011 IEEE International Conference on Mechatronics, 2011, pp. 672–677.
- [42] F. Haugen, The Good Gain method for PI (D) controller tuning, *Tech Teach* (2010) 1–7.

- [43] F. Haugen, The Good Gain method for simple experimental tuning of PI controllers, (2012).
- [44] X. Robert-Lachaine, H. Mecheri, C. Larue, A. Plamondon, Validation of inertial measurement units with an optoelectronic system for whole-body motion analysis, *Med. Biol. Eng. Compu.* 55 (2017) 609–619.
- [45] L. Zhou, E. Fischer, C. Tunca, C.M. Brahms, C. Ersoy, U. Granacher, B.J.S. Arnrich, How we found our IMU: Guidelines to IMU selection and a comparison of seven IMUs for pervasive healthcare applications, 20 (2020) 4090.
- [46] S.K. Hanneman, Design, analysis and interpretation of method-comparison studies, *AACN Adv. Crit. Care* 19 (2008) 223.
- [47] S. Park, S.J.S. Yoon, Validity evaluation of an inertial measurement unit (IMU) in gait analysis using statistical parametric mapping (SPM), 21 (2021) 3667.
- [48] M. Sarshar, S. Polturi, L.J.S. Schega, Gait phase estimation by using LSTM in IMU-based gait analysis—Proof of concept, 21 (2021) 5749.
- [49] Z. Zhou, Z. Zhang, S. Mo, J. Wu, H.J.M. Fourati, Online calibrated, energy-aware and heading corrected pedestrian navigation with foot-mounted MARG sensors, 206 (2023) 112268.
- [50] L. Ruiz-Ruiz, F. Seco, A. Jiménez, S. García, J.J. García, Evaluation of gait parameter estimation accuracy: a comparison between commercial IMU and optical capture motion system, in: 2022 IEEE International Symposium on Medical Measurements and Applications (MeMeA), IEEE, 2022, pp. 1–2.
- [51] D. Renggli, C. Graf, N. Tachatos, N. Singh, M. Meboldt, W.R. Taylor, L. Stieglitz, M. J.F.i.p. Schmid Daners, Wearable inertial measurement units for assessing gait in real-world environments, 11 (2020) 90.